P- ISSN 1991-8941 E-ISSN 2706-6703 *Journal of University of Anbar for Pure Science (JUAPS)* Open Access
2017,11 (1) :39-46

Structural and Optical Properties of In_2O_3 and Indium Tin Oxide Thin Films

Iftikhar M. Ali * , Maisam A. Al-Jenabi**

*College of Science, University of Baghdad.
** College of Science , University of Anbar

ARTICLE INFO

Received: 05 / 02 /2017
Accepted: 15 / 05 /2017
Available online: 00/00/0000
DOI: 10.37652/juaps.2017.141530

Keywords:
In_2O_3,
SnO_2 ,
ITO,
spin coating,
seed layer.

ABSTRACT

The present paper discusses the structural and optical properties of In_2O_3 and ITO thin film growing on glass and silicon substrates by assistant microwave irradiation on seeded layer nucleated by spin coating technique. X-ray diffraction study shows that the films have cubic structure. Morphology analysis was studied by atomic force microscopy (AFM) and reveals that the grain size of the prepared thin film is approximately (62.56-76.66)nm , with a surface roughness of (0.447-1.25) nm as well as root mean square of (0.532-1.44)nm for pure In2O3 and ITO films. Optical characteristics were studied and observed that the transmission value was more than 90 % at the visible wavelength range. The direct energy gap (Eg) was found to be between (3.7-2.6) eV, which decreased significantly with increasing Sn contents.

I. INTRODUCTION

The study and application of thin film technology is entirely entered in to almost all the branches of science and technology. Present study which describes the synthesis and study of structural and optical characteristics of Indium Tin Oxide is really more interesting for researchers due to its vast applications. Due to the properties like reflectivity, transparency, low electrical sheet resistance etc.

* Corresponding author at: College of Science , University of Anbar
.E-mail address:

ITO thin films has immense applications such as photovoltaic cell in transistors, transparent conductive electrode for solar cell photochemical and photoconductive devices in liquid crystal display[1] gas sensor devices[2,3] organic light emitting diodes (OLED)[4,5]. Till today so many methods were adopted to synthesize doped or un-doped ITO films such as R.F. Magnetron Co-sputtering, Thermal Evaporation, Chemical Vapor Deposition, Laser Pulse deposition, sol-gel, Spray Pyrolysis and spin coating technique[6-8]. ITO crystallizes cubic structure[9,10] with lattice constant of a= 10.09 Å. It is found that In_2O_3 nanostructure has direct band gap equal to 3.94 eV, which is higher than the bandgap energy of bulk In_2O_3 (3.6 eV) due to the quantum confinement effect[11,12] with high chemical and mechanical stabilities[13] and is more transparent in the region of visible spectrum due to high band gap. The high electrical conductivity of a TCO results from the presence of atomic-scale defects, which for n-type semiconductors, bring in donors that increase the electron population.

The specific types of atomic-scale defects for a given TCO depend on the specific oxide and its synthesis. They may include oxygen vacancies, cation vacancies, oxygen interstitials, cation interstitials, impurity dopants, cation and anion anti-sites, and defect complexes, which consist of a combination of two or more point defects[5,14].

In this paper, we report the growth of nanostructured thin films of Indium Tin Oxide by assistant microwave irradiation on seeded layer nucleated by spin coating method and this proposed preparation method has never used a PVA-$In(OH)_3$-$Sn(OH)_4$ nanocomposite seed layer to synthesize ITO nanostructures.

II. EXPERIMENTAL

Pure In_2O_3 and Indium Tin Oxide thin films at different ratios of Sn:In which are (0, 10:90, 20:80, 30:70, and 50:50) wt/wt% were prepared by spin coating technique deposited onto silicon and glass substrates. Chemical solutions were prepared by mixing 0.1 M aqueous solutions of $InCl_3$ and $SnCl_4$ at the above ratios using a magnetic stirrer, then they have been added to 1.5g PVA at 80 ^{0}C for 2h, then the resultant solutions have been spin coated on substrates at 1500 rpm for 1min.

This step was repeated several times to obtain the desired thickness for seed layer. Then 0.05 M of $InCl_3$ and $SnCl_4$ at the above ratios were mixed with 0.05 M of hexamine were mixed using magnetic stirrer for 1min prior the seeded substrates have been aligned vertically inside solution which were irradiated in microwave oven at 220W for 1h.

Then washing the substrates with distilled water to remove any non-reacted materials, then dried in oven at 100^{0}C for 30min. After that, the films were been ready to be characterized. The structural properties were determined by X-ray diffraction (XRD- 6000 Labx, supplied by Shimadzu, X-ray source is Cu). Film morphology was analyzed by atomic force microscope (AFM)-type (CSPM). The optical absorption and transmission spectra were obtained using a UV-VIS spectrophotometer (6800 JENWAY, Germany) within the wavelength range of (300-1100)nm.

III . RESULTS AND DISCUSSION

The structure of the prepared ITO thin films were investigated by XRD. Figure (1) shows the plot between (2Θ) versus diffracted ray intensity. The major diffraction peaks at 2Θ = (30.2590, 35.4790 and 51.2300), for pure In_2O_3, thus, the experimental results proved that the polycrystalline nature of the prepared samples as depicted in Figure (1).

The presence of tin has been detected by observation peaks at 2Θ = (26.2540, 33.8670, 37.9900 and 51.8340). The result corresponds with that described by H. A. Mohamed [15]. Moreover, an decreased in the main peak intensity is observed in the presence of tin.

A comparison with ASTM card (96-101-0589) and (96-210-4744), reveals that the ITO thin film exhibits a cubic crystal structure with a preferred orientation (222) for In_2O_3 and (110) for SnO_2, this results agree with that reported by Ju-O Parket al [17]. The crystalline size (D) is determianed from main pack at 2Θ=(30.2590) and found to be equal to (13.6-18.9) nm as shown in Table (1) which based on Scherer formula which is[15]:

$$(D = k\lambda/(\beta Cos(\theta) - - - - - (1)$$

where k is a correction factor=0.89, β is the full width at half maximum (FWHM) in radian.

When the addition rate of Tin increases, the phase of SnO_2 will appear as shown in figure (1) with a preferred orientation (110) for SnO_2 at 2θ=26.5263° which intensity is higher than that for pure In_2O_3 at Sn:In equals 50:50 wt% ratio. It is clear that the addition ratios did not change the direction of crystalline growth of the dominant planes (preferred orientation), where growth continues towards (222) direction for In_2O_3, which is attributable to the Drift model (Survival of the fastest) [16].

An increase in the full width at half maximum (FWHM) and which consequently leads to a decrease in grain size, according to Scherer's formula equation with increasing in the addition ratio with Sn as a comparison of pure Indium oxide thin films, which indicates that the deposited atoms of these films going towards nanostructure.

There was a small shift toward a small angle of diffraction, (to the left of diagram), causing compression in the unit cell because of the ionic radius of the element Sn (0.69Å) [17] smaller than the In (0.80Å) [17], which leads to the atoms of Sn take up substitutional sites in order of Indium crystalline lattice..

Figure (2) displays AFM image of the films at (pure, 10, 20, 30 and 50 wt%). It shows the presence of homogenous grains throughout the film. The grain size of this film is (62.56-76.66) nm for the described different concentrations.

The grain size, root mean square (RMS) and roughness of these films are shown in Table 2. The root mean square and roughness (R) are equal to (1.44, 2.29, 1.63, 1.63, and 0.532) nm, (1.25, 1.96, 1.42, 1.37, and 0.477) nm respectively. Therefore, the film roughness decreases with decreasing of grain size.

Figure (3) observes the absorption (A), transmission (T), and energy gab (E_g) which have been obtained by UV/Vis from (300-1100) nm. Figure (3a) shows the absorption edge for pure In_2O_3 starts with (340) nm reveals that the nanocrystalline effect of the films. also absorption edge of Sn doping indium oxide films shift toward the low energy (red shift). The experimental result agrees with that reported by H.

Ibrahem and M. Moghdad [18] and Ju-O Parket et al [19].

The optical transmittance of Sn-doped In_2O_3 thin films in the visible region is depicted in Figure (3b).

It can be noticed that when the film is pure In_2O_3, the transmittance is about 90% whereas transmittance decreases with Sn addition. Decreasing of the transmittance after Sn addition is owing to increment absorption coefficient of films.

The optical band gap of ITO films is shown in Figure (3c) and is compared with the band gap value for pure indium oxide from the plot of $(\alpha h\upsilon)^2$ as a function of photon energy (hυ) according to Tauc formula represented in the following Eq. (2) for direct band gap semiconductors [20],

$$(\alpha h\upsilon)^2 = A\left(h\upsilon - E_g\right) \text{- - - -} (2)$$

where α is the absorption coefficient, A is a constant, E_g is the optical energy gap, υ is the incident photon frequency, and h is Planck constant. The values of E_g are tabulated in Table 3.

It is evident from the mentioned figure that the energy gap of pure In_2O_3 is equal to 3.7 eV while the energy gap significantly decreases with increasing of Sn concentration.

As a matter of fact, the energy gap is found to be 3.1eV at 10% Sn concentration. That is more clear that when Sn-doped is increased to 20 %, the energy gap is decreased to 2.6 eV. This can be attributed to the fact that the energy gap of Sn oxide is less than the energy gap of In_2O_3 and these results correspond with that reported at ref. [21,22].

Conclusions

Indium Tin oxide thin films were prepared by spin coating method. The X-ray diffraction shows the polycrystalline nature of deposited films with cubic structure. The crystallite size of the film was calculated using Debye-Scherer formula is varies from 13.6-18.9 nm.

The AFM images show homogenous films with grain sizes ranging from (62.56-76.66) nm. The calculated band gap energies decrease with the increase of Sn concentration, as a result of the occurrence of additional energetic levels in the forbidden gap.

Acknowledgements

The authors acknowledge the University of Baghdad, College of Science, department of physics for support to this research.

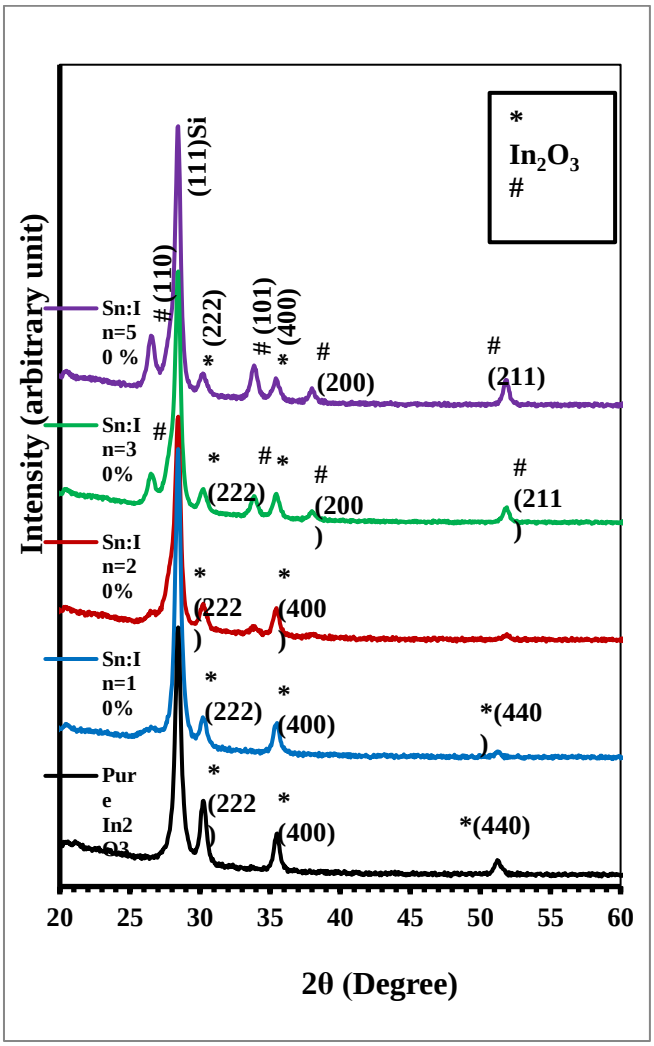

Fig. 1. x-ray diffraction patterns of ITO thin films

Table 1. Average Crystallite size (D), inter planer spacing (d) and FWHM for ITO

n:In	2θ (Deg.)	FWHM (Deg.)	d_{hkl} Exp.(Å)	D (nm)	hkl	d_{hkl} Std.(Å)	Phase	Card No.
0%	30.2590	0.4350	2.9513	18.9	(222)	2.9214	In_2O_3	96-101-0589
	35.4790	0.4844	2.5281	17.2	(400)	2.5300	In_2O_3	96-101-0589
	51.2300	0.4880	1.7818	18.1	(440)	1.7890	In_2O_3	96-101-0589
10%	30.2460	0.5396	2.9526	15.3	(222)	2.9214	In_2O_3	96-101-0589

	35.4660	0.5124	2.5290	16.3	(400)	2.5300	In_2O_3	96-101-0589
20%	30.2330	0.5675	2.9538	14.5	(222)	2.9214	In_2O_3	96-101-0589
	35.4530	0.5678	2.5299	14.7	(400)	2.5300	In_2O_3	96-101-0589
30%	26.5263	0.5820	3.3575	14.0	(110)	3.3498	SnO_2	96-210-4744
	30.2265	0.5840	2.9544	14.1	(222)	2.9214	In_2O_3	96-101-0589
	33.8721	0.5680	2.6443	14.6	(101)	2.6439	SnO_2	96-210-4744
	35.4465	0.5814	2.5304	14.4	(400)	2.5300	In_2O_3	96-101-0589
	37.9985	0.5720	2.3661	14.7	(200)	2.3686	SnO_2	96-210-4744
	51.9015	0.5040	1.7603	17.5	(211)	1.7642	SnO_2	96-210-4744
50%	26.5240	0.6006	3.3578	13.6	(110)	3.3498	SnO_2	96-210-4744
	30.2200	0.5950	2.9550	13.8	(222)	2.9214	In_2O_3	96-101-0589
	33.8670	0.5643	2.6447	14.7	(101)	2.6439	SnO_2	96-210-4744
	35.4400	0.5950	2.5308	14.0	(400)	2.5300	In_2O_3	96-101-0589
	37.9900	0.5931	2.3666	14.2	(200)	2.3686	SnO_2	96-210-4744
	51.8340	0.6230	1.7624	14.2	(211)	1.7642	SnO_2	96-210-4744

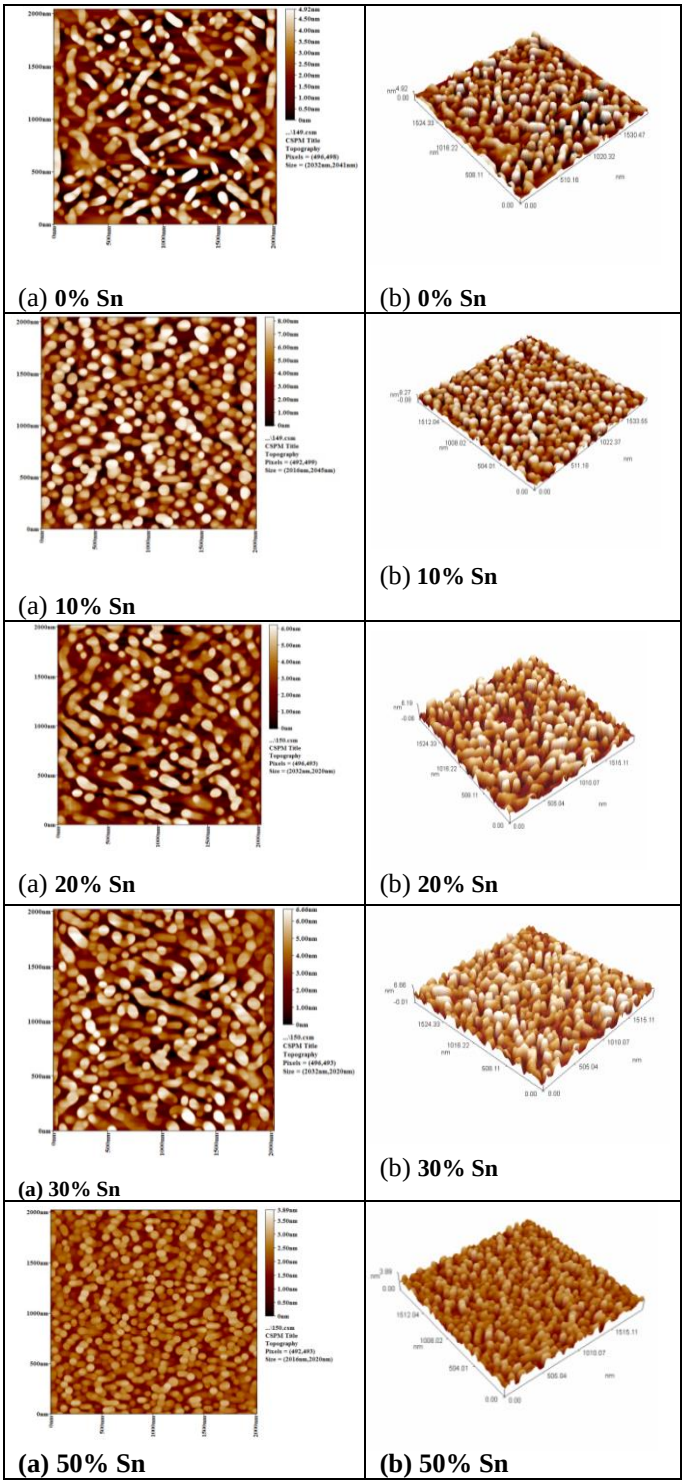

Fig. 2. The atomic force microscope (a) 2-D and (b) 3-D Images of prepared films

Table 2: The Average gain sizes and Roughness average for undoped and doped In_2O_3 films.

%SnO_2	Average diameter (nm)	Roughness (nm)	Peak-Peak (nm)	(r.m.s.) nm
0	71.94	1.25	4.91	1.44
10	73.84	1.96	8.33	2.29
20	76.66	1.42	6.25	1.63
30	62.56	1.37	6.67	1.63
50	64.09	0.447	2.53	0.532

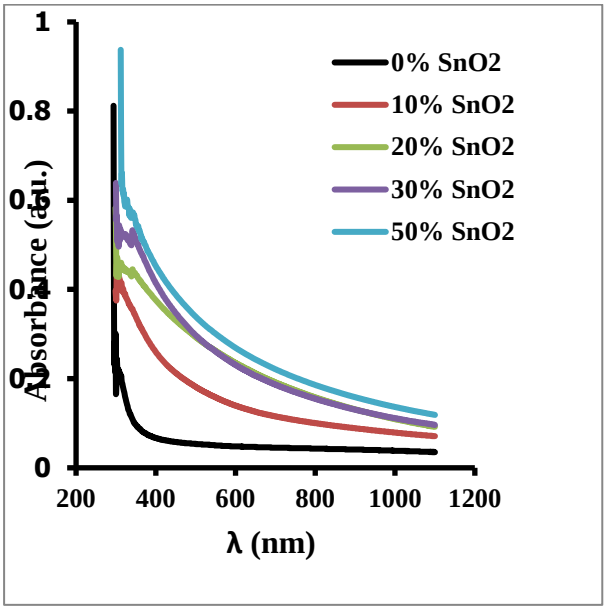

Fig. 3a The absorption of prepared films

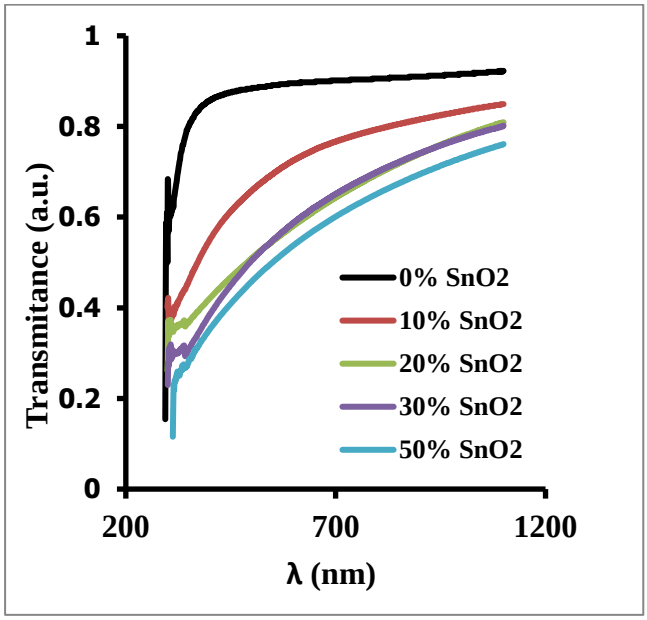

Fig. 3b The transmittance of prepared films

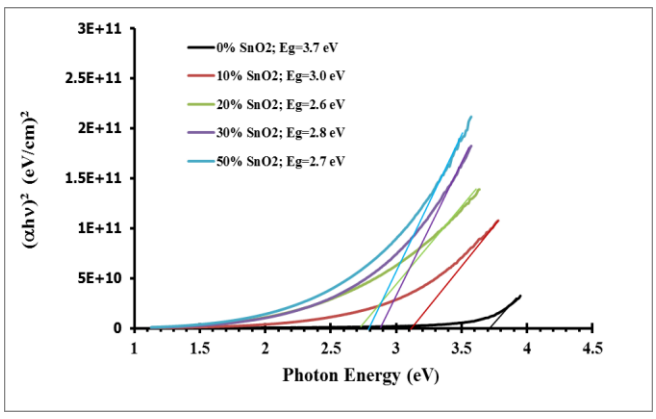

Fig. (3c) Tauc plot of ITO films

Table 3 Band gap energies calculated from Tauc method

% Sn	0	10	20	30	50
E_g(ev)	3.7	3.1	2.6	2.8	2.7

References

[1] Solieman A. and Aegerter M., "Modeling of optical and electrical properties of In2O3:Sn coatings made by various techniques", Thin Solid Films (2006) 502(1/2): 205–211.

[2] Ahmad M. Z., Chang J., Sadek A. Z., "Non-aqueous synthesis of In2O3nanoparticles and its NO2 gas sensing properties", IMCS– The 14th International Meeting on Chemical Sensors (2012)1060-1063.

[3] Daoudi K, Canut B, Blanchin M. G., Sandu C. S., Teodorescu V. S., Roger J. A., "Tin-doped indium oxide thin films deposited by sol-gel dip-coating technique", Materials Science and Engineering (2002) 21: 313–317.

[4] Ishibashi K., Watabe K., Sakurai T., Okada O., Hosokawa N., "Large area deposition of ITO films by cluster type sputtering system", J. Non-Crystalline Solids (1997) 218: 354–359.

[5] Sivaranjani V. and Philominathan P., "Influence of Substrate Temperature on Physical Properties of Nanostructured Ti Doped In2O3 Thin Films by a Simplified Perfume Atomizer Technique", Int. J. Thin. Fil. Sci. Tec. (2015) 4, No. 3, 219-225.

[6] Chen B. J., Sun X.W., Tay B. K., "Fabrication of ITO thin films by filtered cathodic vacuum arc deposition", Mater. Sci. Eng. B. (2004)106: 300-304.

[7] Cho H. J., Hwangbo C. K.,"Optical inhomogeneity and microstructure of ZrO2 thin films prepared by ion-assisted deposition", Appl. Opt. (1996)35: 5545- 5552.

[8] Choi J., B., Kim J. H., Jeon K. A., Lee S. Y.,"Properties of ITO films on glass fabricated by pulsed laser deposition", Mater. Sci. Eng., B. (2003) 102: 376-379.

[9] Chou T. H., Cheng K. Y., Chang T. L., Ting C. J., Hsu H. C., Wu C. J., Tsai J. H., Huang T. Y., "Fabrication of antireflection structure on TCO film for reflective liquid crystal display", Micro electron. Eng. (2009) 86: 628-831.

[10] El Amrani A., Hijazi F., Lucas B., Bouclé J., Aldissi M., "Electronic transport and optical properties of thin oxide films", Thin Solid Films (2010) 518: 4582- 4585.

[11] Majeed M.A., Khan W. , Ahamed M., Alhoshan M. "Structural and optical properties of In2O3 nanostructured thin film", Materials Letters (2012) 79, 119–121.

[12] Beena D., Lethy K. J., Vinodkumar R., Detty A. P., Mahadevanpillai V. P. , Ganesan V. "Photoluminescence in Laser Ablated Nanostructured Indium Oxide Thin Films" Optoelectronics and Advanced Materials – Rapid Communications Vol. 5, No. 1, 2011, 1–11.

[13] Fakhri M. A., "Effect of Substrate Temperature on Optical and Structural Properties of Indium Oxide Thin Films Prepared by Reactive PLD Method", Eng. & Tech. Journal (2014)Vol.32 (A), No.5,1323-1330.

[14] González G.B., "Investigating the Defect Structures in Transparent Conducting Oxides Using X-ray and Neutron Scattering Techniques", Materials (2012) 5, 818-850.

[15] Mohamed H. A., "Effect of substrate temperature on physical properties of In2O3:Sn films deposited by e-beam technique", Int. J. Physical Sciences (2012) 7(13), 2102 - 2109.

[16] Kachkanov V., Leung B., Song J., Zhang Y., Tsai C., Yuan G., Han J. and O,Donnell K., "Structural Dynamics of GaN Microcrystals in Evolutionary Selection Selective Area Growth probed by X-ray Microdiffraction", Scientific Reports (2014) 4, Article number: 4651.

[17] Shannon R. D., "Revised effective ionic radii and systematic studies of interatomic distances in halides and chalcogenides". Acta Crystallogr A. (1976) 32: 751–767.

[18] Ibrahem H., Moghdad M."Preparation of ITO thin film by Sol-Gel method", Int. J. Electrical Engineering (2013) 1(6)18-22.

[19] Park J., Lee J., Kim J., Cho S., Cho Y., "Crystallization of indium tin oxide thin films prepared by RF-magnetron sputtering without external heating" ,Thin Solid Films (2005) 474, 127–132.

[20] Tauc J., Grigorovici R., Vancu A., "Optical properties and electronic structure of Germanium", Phys. Stat. Sol., 15, p.627 (1966).

[21] Marikkannu S., Ayeshamariam A., Vidhya V. S., Sethupathy N., " Preparation of Characterizations of ITO Thin Films with Different Sn Concetration by Jet Nebulizer Technique", J. Photonics and Spintronics (2014) 3 (2) 4-9.

[22] Fallaha H. R., Ghasemia M., Hassanzadehb A., "The effect of deposition rate on electrical, optical and structural properties of tin-doped indium oxide (ITO) films on glass at low substrate temperature", Physica B. (2006) 373: 274- 279.

P- ISSN 1991-8941 E-ISSN 2706-6703 *Journal of University of Anbar for Pure Science (JUAPS)* Open Access
2017,11 (1) :39-46

الخصائص التركيبية والبصرية لأغشية أوكسيد الأنديوم–أوكسيد القصدير الرقيقة

افتخار محمود علي ميسم احمد الجنابي

الخلاصة:

في هذا البحث تم مناقشة الخواص التركيبية والبصرية لأغشية In_2O_3 و ITO ، تم انماء هذه الاغشية على قواعد ترسيب من الزجاج والسليكون بواسطة استعمال اشعاع المايكروويف على طبقة البذرة بتقنية الطلاء البرمي. وعن طريق حيود الاشعة السينية بينت ان الاغشية تمتلك تركيب متعدد التبلور طور مكعبي. تم دراسة مورفولوجية السطح بواسطة مجهر القوة الذرية (AFM) حيث وجد ان الحجم الحبيبي للأغشية الرقيقة المحضرة In_2O_3 و ITO يساوي تقريبا (62.56 – 76.66)nm وخشونة السطح (0.447 – 1.25)nm ومتوسط الجذر التربيعي (0.532 – 1.44)nm. تم دراسة الخصائص البصرية ولوحظ ان قيمة النفاذية اكثر من 90% في مدى الطول الموجي المرئي. ان فجوة الطاقة المباشرة (Eg) كانت قيمتها بين (3.7 – 2.6) eV والتي انخفضت بشكل ملحوظ عند زيادة نسب القصدير .